JOURNAL OF GUIDANCE, CONTROL, AND DYNAMICS
Vol. 17, No. 5, September–October 1994

Novel Three-Dimensional Differential Game and Capture Criteria for a Bank-to-Turn Missile

A. Segal
Israel Aircraft Industries, Inc., Lod 70350, Israel
and
T. Miloh*
Tel-Aviv University, Tel-Aviv 69978, Israel

The formulation and solution of a new pursuit-evasion differential game are presented in this paper. Considering the game as a "game of kind," in Isaacs' terminology, capture criteria are established in terms of the game parameters for a faster bank-to-turn pursuer engaging a slower but more maneuverable evader in three-dimensional space. This paper covers the range of players' speed ratio for which the barrier surface is of the "classical" type, i.e., with tangential termination on the target set.

I. Introduction

CONVENTIONAL aircraft and many of the high-speed missiles are of the bank-to-turn type. A three-dimensional encounter between a fast pursuer of this type and a highly maneuverable evader (which is modeled as a "pedestrian" à la Isaacs[1]) is considered. The (constant) speeds of the pursuer and evader are denoted by V_p and V_E, respectively. The pursuer has a minimal turning radius[2] in his pitch plane denoted by R and a limited roll rate denoted by ω_s. Capture is effected whenever the pursuer-evader instantaneous separation is less than l_c, which is considered here as the game performance index.

In many realistic pursuit-evasion situations it is desired to force the evader into the pursuers' pitch plane just prior to game termination. The pursuer is capable of steering the "end game" into his preferable pitch plane only if he or she can apply a roll rate that is larger than some critical value ω_c. In this case, the pursuer executes a three-stage maneuver consisting of two hard turns in opposite directions combined with a unidirectional roll maneuver and then finally a zero roll-rate (ω_s-universal curve) hard turn until game termination. For a roll rate that is lower than ω_c but still larger than some marginal value ω_m, the pursuer executes a two-stage maneuver consisting of only the first two above-mentioned hard turns, thus steering the dynamic system into the target set. These optimal pursuit-evasion maneuvers and the associated critical capture radii are also discussed in a former paper.[3] If the maximum available pursuer's roll rate is even less than ω_m, the pursuer executes a four-stage maneuver consisting of the previous two hard turns followed by an inverted roll-rate hard turn and finally by a straight-line motion with both controls set to zero (u, ω_s; universal line). In this case the evader changes his or her attitude controls abruptly once the pursuer's wing plane is reached, thus steering the end game into the pursuer's unfavorable yaw plane.

The limiting cases of $\omega_s \to 0$ or $\omega_s \to \infty$ are of particular interest since, clearly, the inequality $l_c(\omega_s \to \infty, V_p, V_E, R) < l_c(\omega_s V_p, V_E, R) < l_c(\omega_s \to 0, V_P, V_E, R)$, holds for the capture radius and we are interested in the degradation of l_c as a function of the pursuer's finite roll rate ω_s. It is shown that by letting $\omega_s \to \infty$, the present differential game—(DG) degenerates into the familiar "homicidal chauffeur" game for which the capture condition has been already established.[1] The asymptotic behavior of l_c in the limiting case $\omega_s \to 0$ is also presented.

The novel DG equations are derived in Sec. II. A closed-form analytic solution for the optimal trajectories and costate variables is presented in Sec. III. The critical capture radius l_c for the whole range of ω_s and a wide range of players' speed ratio $\gamma = V_E/V_p < 1$ is established in Sec. IV. Some numerical examples are presented in Sec. V and concluding remarks are made in Sec. VI.

The solutions presented in this paper provide an analytical tool for assessing the general performance capabilities of a bank-to-turn pursuer and may be considered as a first attempt toward generalizing the two-dimensional capturability criteria of Refs. 1, 4, and 5 for a genuine three-dimensional pursuit-evasion encounter.

Received Feb. 11, 1993; revision received Nov. 9, 1993; accepted for publication Feb. 16, 1994.

*Professor, Faculty of Engineering.

II. New Differential Game

As a reference frame we employ the pursuer's body-fixed axes and describe the three-dimensional relative motion of the evader with respect to the pursuer (reduced space formulation) as depicted in Fig. 1. The radius vector $\boldsymbol{r}_{EP}$ denotes the instantaneous position of E (evader) relative to P (pursuer):

$$\boldsymbol{r}_{EP} = (x, y, z) \tag{1}$$

Here the E inertial velocity vector (assumed to have constant magnitude) resolved in the P body axes is given by

$$\boldsymbol{V}_E = V_E(\cos\theta\cos\psi, \cos\theta\sin\psi, -\sin\theta) \tag{2}$$

where θ and ψ are the evader's two heading controls.

The angular velocity of the body-axes triad is given by

$$\boldsymbol{\Omega} = \left(\omega_s, \frac{V_p}{R}u, 0\right) \tag{3}$$

where ω_s is the pursuer's bounded roll rate ($-\omega_{s,\max} \le \omega_s \le \omega_{s,\max}$) and u is the nondimensional parameter ($-1 \le u \le 1$) representing the pursuer's pitch rate. Finally, V_p is the pursuer's constant speed, and R is his or her minimal curvature radius in the pitch plane (x-z plane).

It is further assumed that the pursuer has a limited (bounded) yaw rate; for this reason it is advantageous for the pursuer to perform a bank-to-turn maneuver in order to change his or her direction in three-dimensional space. This is indeed the situation for conventional aircraft and high-speed missiles.

Thus, the absolute velocity of the evader, expressed in terms of the pursuer body-fixed coordinate system, is

$$\boldsymbol{V}_E = \boldsymbol{V}_p + \dot{\boldsymbol{r}}_{EP} + \boldsymbol{\Omega} \times \boldsymbol{r}_{EP} \tag{4}$$

where the time differentiation of $\boldsymbol{r}_{EP}$ is done relative to the inertial system. Using dimensionless representation, one gets the following kinematic system:

$$\begin{bmatrix}\dot{x}\\ \dot{y}\\ \dot{z}\end{bmatrix} = \begin{bmatrix}0 & 0 & -u\\ 0 & 0 & \omega_s\\ u & -\omega_s & 0\end{bmatrix}\begin{bmatrix}x\\ y\\ z\end{bmatrix} + \gamma\begin{bmatrix}\cos\theta\cos\psi\\ \cos\theta\sin\psi\\ -\sin\theta\end{bmatrix} - \begin{bmatrix}1\\ 0\\ 0\end{bmatrix} \tag{5}$$

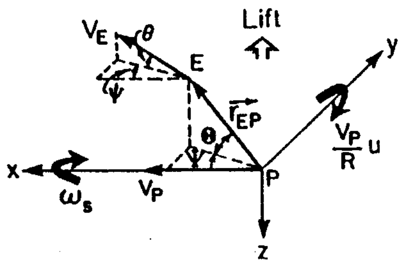

Fig. 1 Relative geometry and state variables.

where

$$x \to \frac{x}{R}, \qquad y \to \frac{y}{R}, \qquad z \to \frac{z}{R}, \qquad t \to \frac{tV_p}{R}$$

$$\omega_s \to \frac{\omega_s}{V_p/R} \qquad \omega_{s,\max} \to \frac{\omega_{s,\max}}{V_p/R} \tag{6}$$

$$r_{EP} \to \frac{r_{EP}}{R}, \qquad \gamma \triangleq \frac{V_E}{V_p} < 1$$

The spherical coordinates of E with respect to P are (see Fig. 1)

$$(x, y, z) = r(\cos\Theta\cos\Psi, \cos\Theta\sin\Psi, -\sin\Theta)$$

$$r = |\boldsymbol{r}_{EP}| \tag{7}$$

Let us next define the spherical target set by

$$r^2 = x^2 + y^2 + z^2 = l^2 \tag{8}$$

which implies that the three problem parameters of this new DG are $\gamma < 1$, $l > 0$, and $\omega_{s,\max} > 0$. One of the interesting results of the analytic solution of such a three-dimensional pursuit-evasion DG is the establishment of a capture criterion in the form of a relationship between the minimum capture radius l_c and the kinematic game parameters γ and ω_s.

The condition for a penetration of the target set by the evader is determined by the following inequality:

$$\max_{\theta,\psi} \boldsymbol{\nu}\cdot\boldsymbol{r}_{EP} \le 0 \tag{9}$$

where $\boldsymbol{\nu}$ is the outward pointing normal to the target set. It follows that (see also Ref. 3)

$$\theta_f = \Theta_f, \qquad \psi_f = \Psi_f \tag{10}$$

$$\cos\Theta_f \cos\Psi_f \ge \gamma \tag{11}$$

where the subscript f is used here to denote termination of the game.

The usable part (UP) is therefore a spherical cap, and the boundary of the usable part (BUP) is a circle—the circumference of the cap's basis.

Let us denote the components of the outward pointing normal to the Barrier surface by $(\lambda_x, \lambda_y, \lambda_z)$ and express the corresponding Hamiltonian as

$$H = \gamma \max_{\theta,\psi}(\lambda_x \cos\theta\cos\psi + \lambda_y \cos\theta\sin\psi - \lambda_z \sin\theta)$$
$$+ \min_{|u|\le 1}[u(\lambda_z x - \lambda_x z)] + \min_{|\omega_s|\le\omega_{s,\max}}[\omega_s(\lambda_y z - \lambda_z y)] - \lambda_x = 0 \tag{12}$$

which is supplemented by the following adjoint equations:

$$(\dot\lambda_x, \dot\lambda_y, \dot\lambda_z) = (-u\lambda_z, \omega_s\lambda_z, u\lambda_x - \omega_s\lambda_y) \tag{13}$$

The first form of the main equation (12) and the lemma on circular vectograms lead to

$$\lambda_x = \lambda\cos\theta\cos\psi, \qquad \lambda_y = \lambda\cos\theta\sin\psi, \qquad \lambda_z = -\lambda\sin\theta \tag{14}$$

where, for convenience, we may choose $\lambda = 1$. The Hamiltonian (12) also renders the following relationships for the pursuer's optimal controls:

$$u = \operatorname{sgn}(\lambda_x z - \lambda_z x) = \operatorname{sgn}(S_1)$$
$$\omega_s = \omega_{s,\max}\operatorname{sgn}(\lambda_z y - \lambda_y z) = \omega_{s,\max}\operatorname{sgn}(S_2) \tag{15}$$

where S_1 and S_2 denote the respective switching functions. Substitution of (14) and (15) into (12) yields the main equation (ME_2):

$$\gamma - \lambda_x - |S_1| - \omega_{s,\max}|S_2| = 0 \tag{16}$$

III. Analytic Solution for State and Costate Variables

In view of the optimality conditions (14) and (15), the two sets of differential equations (5) and (13) may be transformed into a set of six linear and coupled differential equations, the solution of which may be expressed as

$$\lambda_x(\tau) = -\frac{u}{\omega}a\cos\omega\tau + \frac{u}{\omega}b\sin\omega\tau + \frac{\omega_s}{\omega}c$$
$$\lambda_y(\tau) = \frac{\omega_s}{\omega}a\cos\omega\tau - \frac{\omega_s}{\omega}b\sin\omega\tau + \frac{u}{\omega}c \tag{17}$$
$$\lambda_z(\tau) = a\sin\omega\tau + b\cos\omega\tau$$

and

$$x(\tau) = -\frac{u}{\omega}f_1(\tau)\cos\omega\tau + \frac{u}{\omega}f_2(\tau)\sin\omega\tau + \frac{\omega_s}{\omega}f_3(\tau)$$
$$y(\tau) = \frac{\omega_s}{\omega}f_1(\tau)\cos\omega\tau - \frac{\omega_s}{\omega}f_2(\tau)\sin\omega\tau + \frac{u}{\omega}f_3(\tau) \tag{18}$$
$$z(\tau) = f_1(\tau)\sin\omega\tau + f_2(\tau)\cos\omega\tau - \frac{u}{\omega^2}$$

where τ is the retrograde nondimensional time, ω is the total pursuer's nondimensional rate of turn, i.e.,

$$\omega^2 \triangleq u^2 + \omega_s^2 \tag{19}$$

a, b, c are constants based on the costate initial conditions, and $f_1(\tau)$, $f_2(\tau)$, $f_3(\tau)$ are linear time functions, which depend on the state and costate initial conditions (see Ref. 3).

According to (15), (17), and (18) we find that for $\tau \to 0^+$, the optimal controls employed by the pursuer just prior to penetration into the BUP are given by

$$\bar u = -\operatorname{sgn}(\lambda_{z_f}) = -\operatorname{sgn}(z_f) = \operatorname{sgn}(\Theta_f)$$
$$\bar\omega_s = \omega_{s,\max}\operatorname{sgn}[\lambda_y \operatorname{sgn}(-z_f)] = -\omega_{s,\max}\operatorname{sgn}(y_f z_f) \tag{20}$$
$$= \omega_{s,\max}\operatorname{sgn}(\Theta_f \Psi_f)$$

Thus, the pursuer always turns on the target set toward the evader so as to decrease y, the relative lateral distance. The evader, on the other hand, runs away from the pursuer and continues to increase y. Maximum values of roll rates $\omega_{s,\max}$, higher than ω_c or less than ω_m, lead to singularities in the sgn functions (20) and to an "end-game trajectory" either along a ω_s-universal curve (with $|u| = 1$ and $\omega_s = 0$) or along a (u, ω_s)-universal line (with $u = \omega_s = 0$) up to game termination on the BUP.

IV. Critical Capture Radius

As long as the distance between the pursuer and the evader is larger than some critical range x_1, the pursuer can always keep the evader directly ahead, whatever the evader does. As the range between players decreases, the evader must choose the right instance to break abruptly toward a new direction in the R^3 space. At this particular break-away point, which is characterized by the initial range x_1, the initial adjoint λ_{x_1} is zero:

$$\lambda_{x_1} = 0 \tag{21}$$

and, in addition,

$$y_1 = z_1 = 0 \tag{22}$$

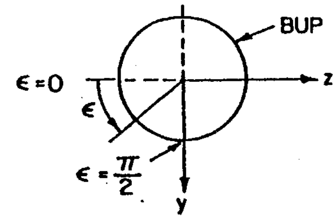

Fig. 2 The BUP angle ϵ.

A two-dimensional analog of such an initial condition has been also employed by Breakwell and Merz[4] in their quest to find a capture criterion for Isaacs' game of two cars.

Starting with the terminal conditions on the BUP, the kinematic equations are solved in the retrogressive sense by moving backward along the optimal trajectory until the point $(x_1, 0, 0)$ is reached. We thus find the critical capture radius l_c as a function of the pursuer's nondimensional roll rate ω_s (actually, the ratio between the roll and pitch rates) and the speed ratio $\gamma(V_E/V_p)$. Without loss of generality, we consider here only those trajectories that terminate on one-quarter of the BUP (see Fig. 2), at which $0 \leq \epsilon \leq \frac{1}{2}\pi$, where ϵ satisfies

$$\epsilon = \tan^{-1}\frac{\sin\Psi_f}{\tan\Theta_f} \tag{23}$$

The existence of a barrier surface that terminates tangentially at the BUP is guaranteed if $\ddot{r}_f \geq 0$, providing there is no penetration into the target set for $t_f > t \geq 0$. Utilizing Eqs. (7), (10), (11), and (23) leads to the following equivalent condition:

$$(l_c\cos\epsilon)^2 + \gamma^2 \leq 1 \tag{24}$$

This condition holds for all values of ω_s and for speed ratios up to $\gamma = 0.721$. In the sequel we will consider all possible cases for which inequality (24) holds. In particular, a distinction is made between cases in which the optimal trajectory leading to the BUP consists of two-, three-, or four-stage maneuvers, where at least one of the players is applying a different (bang-bang) control on each segment.

A. Two-Stage Trajectory

An optimal trajectory that terminates on the BUP at $0 < \epsilon < \frac{1}{2}\pi$ is found to consist of two stages, the first stage starting at $(x_1, 0, 0)$ and terminating at (x_s, y_s, z_s) on a switching line along which $S_1 = 0$. The second stage starts at (x_s, y_s, z_s) and ends at a point (x_f, y_f, z_f) lying on the BUP (see Fig. 3). The switching time is the evolute of the smallest positive root, τ_s, which annuls the switching function $S_1 = \lambda_x z - \lambda_z x$. Thus, τ_s satisfies the following implicit relation:

$$\tau_s = -\frac{1}{\omega_s^2}\frac{\cos\theta_f\cos(\psi_f + 2\alpha)[1-\cos\omega\tau_s] + \sin\theta_f\cos\alpha\sin\omega\tau_s}{\sin\theta_f\cos\omega\tau_s + \cos\theta_f\cos(\psi_f+\alpha)\sin\omega\tau_s} \tag{25}$$

where

$$\alpha \triangleq \tan^{-1}\omega_s \tag{26}$$

We note that ω_s can take on values only in the range $\omega_m \leq \omega_s \leq \omega_c$, where with $\omega_s = \omega_m$, the trajectory terminates at $\epsilon = \frac{1}{2}\pi$ and for $\omega_s = \omega_c$ termination occurs at $\epsilon = 0$. Thus, for a given $\omega_s(\omega_m \leq \omega_s \leq \omega_c)$ the retrogressive time τ_s, the state vector (x_s, y_s, z_s), and the costate vector $(\lambda_{x_s}, \lambda_{y_s}, \lambda_{z_s})$ are all determined from the transversality conditions

$$\begin{aligned} \boldsymbol{x}_s(\tau_s^+) &= \boldsymbol{x}_s(\tau_s^-) \triangleq \boldsymbol{x}_s = (x_s, y_s, z_s) \\ \boldsymbol{\lambda}_s(\tau_s^+) &= \boldsymbol{\lambda}_s(\tau_s^-) \triangleq \boldsymbol{\lambda}_s = (\lambda_{x_s}, \lambda_{y_s}, \lambda_{z_s}) \end{aligned} \tag{27}$$

The new "initial conditions" (actually, the terminal conditions of the first stage) are now obtained as functions of l and ϵ. It should also be noted that τ_s does not explicitly depend on the miss distance l. Based on these new initial conditions, we get the path equations for the first stage of the trajectory and find both $l = l_c$ and ϵ by satisfying Eqs. (21) and (22).

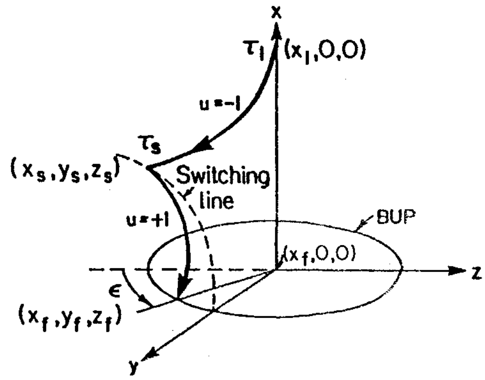

Fig. 3 Two-stage trajectory.

The time traveled along the first stage is the smallest positive root τ_1 that annuls λ_{x_1}, i.e.,

$$\tau_1 = \frac{1}{\omega}\left[\pi + \sin^{-1}\left(\omega_s\frac{c}{d}\right) - \phi\right] \tag{28}$$

where

$$d \triangleq \sqrt{a^2+b^2}, \qquad \phi \triangleq \sin^{-1}\frac{a}{d} \tag{29}$$

Enforcing $z_1 = z(\tau_1) = 0$, we get, for the critical radius,

$$l_c = \gamma(\tau_s+\tau_1) - \frac{a_1\sin\omega\tau_1 + b_1\cos\omega\tau_1 + 1/\omega^2}{a\sin\omega\tau_1 + b\cos\omega\tau_1} \tag{30}$$

where τ_s and τ_1 are given by Eqs. (25) and (28), respectively.

Similarly, using $y_1 = y_1(\tau_1) = 0$ implies that

$$l_c = \gamma(\tau_s+\tau_1) + \frac{c_1 + (\omega_s/\omega)\tau_1 - \omega_s(a_1\cos\omega\tau_1 - b_1\sin\omega\tau_1)}{\omega_s(a\cos\omega\tau_1 - b\sin\omega\tau_1) - c} \tag{31}$$

where a, b, c, a_1, b_1, and c_1 are all constants defined in Ref. 3. By comparing Eq. (30) with Eq. (31), we finally get an implicit equation from which the BUP angle $\epsilon(0 \leq \epsilon \leq \frac{1}{2}\pi)$ can be found, and consequently, the critical capture radius l_c can be determined. Figure 6 presents the criterion $(l_c\cos\varepsilon)^2 + \gamma^2$ as a function of ω_s for three typical values of speed ratio γ. It may be noticed that $\gamma = 0.721$ is the highest value for which a tangential termination barrier still exists for all values of ω_s. Note that there is no ω_s switching along this two-stage trajectory and for this reason the ω_s mentioned above according to Eq. (15) is actually $\omega_{s,\max}$.

B. Three-Stage Trajectory

If the pursuer has a maximum roll rate that is larger than ω_c, then the optimal maneuver consists of three distinct stages: the first stage starts at $(x_1, 0, 0)$ and terminates at (x_s, y_s, z_s) on the switching line; the second stage (a tributary) starts at (x_s, y_s, z_s) and terminates at $(x_B, 0, z_B)$ on the ω_s-universal line (UL); and the third stage (a segment of the ω_s-UL) starts at $(x_B, 0, z_B)$ and ends on the BUP at $(x_f, 0, z_f)$ (see Fig. 4). The UL equations can be obtained (see Ref. 3) by substituting $\omega_s = 0$ and $\lambda_y = y = 0$ in Eqs. (17) and (18), from which one can find the "initial conditions" for the second stage, i.e., $\boldsymbol{x}_B$ and $\boldsymbol{\lambda}_B$ for $\tau = \tau_B$, where τ_B denotes the departure time of the tributary (second stage) from the UL.

By following a similar procedure to the one used in the previous paragraph, we obtain an implicit equation from which we can determine τ_B for a given $\omega_s \geq \omega_c$ as well as the critical capture radius l_c. The switching time τ_s in this case satisfies the following relation:

$$\begin{aligned} \tau_s = {}& -\omega_s^{-2}\{[\sin(\theta_f+\tau_B)\cos\omega\tau_s + \cos(\theta_f+\tau_B)\cos\alpha \\ & \times \sin\omega\tau_s]\}^{-1}\{[\gamma + \cos(\theta_f+\tau_B)\cos 2\alpha](1+\omega_s^2\cos\omega\tau_s) \\ & - \cos(\theta_f+\tau_B)(1+\cos\omega\tau_s) \\ & + \sin(\theta_f+\tau_B)\cos\alpha\sin\omega\tau_s\} \end{aligned} \tag{32}$$

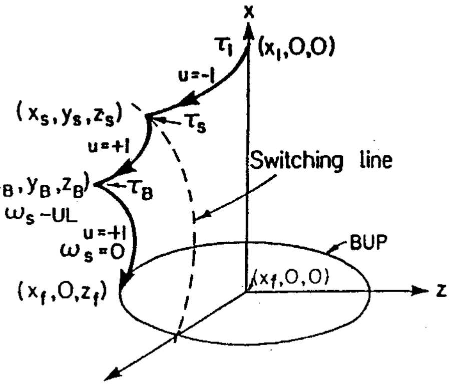

Fig. 4 Three-stage trajectory.

where α is defined by Eq. (26). For $\omega_s = \omega_c$, where $\epsilon = 0$, Eqs. (32) and (25) can be shown to be identical.

Starting with the initial conditions x_B and λ_B at τ_B, traveling backward along the second-stage trajectory and substituting $\tau = \tau_s$ from (32), we get the necessary initial conditions for the first stage, x_s and λ_s, in terms of the parameters l and τ_B.

The time traveled along the first stage is given by Eq. (28). Letting $z_1 = z(\tau_1) = 0$, Eq. (30) is replaced here by

$$l_c = \gamma(\tau_B + \tau_s + \tau_1) - \frac{a_1 \sin\omega\tau_1 + b_1 \cos\omega\tau_1 + 1/\omega^2}{a \sin\omega\tau_1 + b \cos\omega\tau_1} \tag{33}$$

Next, we let $y_1 = y(\tau_1) = 0$, and get, instead of Eq. (31),

$$l_c = \gamma(\tau_B+\tau_s+\tau_1) + \frac{c_1 + (\omega_s/\omega)\tau_1 - \omega_s(a_1 \cos\omega\tau_1 - b_1 \sin\omega\tau_1)}{\omega_s(a \cos\omega\tau_1 - b \sin\omega\tau_1) - c} \tag{34}$$

where a, b, c, a_1, b_1, and c_1 are again some new constants defined in Ref. 3.

By comparing Eq. (33) with Eq. (34) we get an implicit equation from which τ_B can be derived, and then, by invoking Eq. (33) or (34), the critical capture radius l_c can be determined. As previously mentioned, $\omega_s = \omega_{s,\max}$ along the first two stages and on the third segment (UL) $\omega_s = 0$.

If the pursuer has an infinite roll rate, it can be shown that the condition $\lim_{\omega_s\to\infty} S_1 = 0$ leads to

$$\lim_{\omega_s\to\infty} \omega\tau_s = \frac{\pi}{2} \tag{35}$$

For this degenerate case the coefficients a, b, c, and d are given by

$$a = \sin(\theta_f + \tau_B), \qquad b = 0, \qquad c = \cos(\theta_f + \tau_B)$$

$$d \triangleq \sqrt{a^2 + b^2} = |\sin(\theta_f + \tau_B)| \tag{36}$$

According to (28), there exists a finite τ_1 only if the argument of $\sin^{-1}$ satisfies

$$\lim_{\omega_s\to\infty} \left|\frac{\omega_s c}{d}\right| \le 1 \tag{37}$$

from which, by substituting Eq. (36), we get

$$\lim_{\omega_s\to\infty} (\theta_f + \tau_B) = \frac{\pi}{2} \tag{38}$$

Using the relationship $\theta_f = \cos^{-1}\gamma$ in Eq. (38), one gets, for $\omega_s \to \infty$,

$$\tau_B = \sin^{-1}\gamma \tag{39}$$

Following Eq. (28), it is also clear that $\tau_1 = 0$ for $\omega_s \to \infty$. Thus, the time to go for an infinite roll rate is

$$t_{go} = \tau_B + \tau_S + \tau_1 = \tau_B = \sin^{-1}\gamma \tag{40}$$

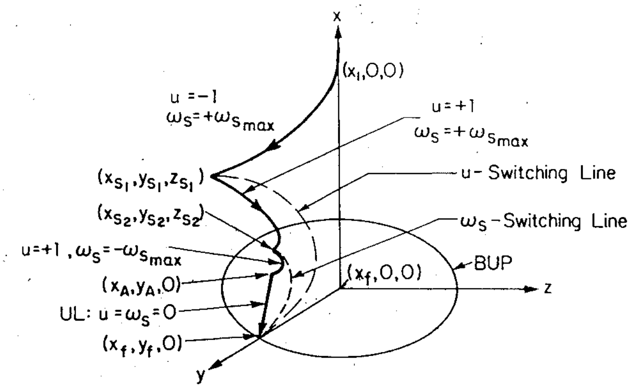

Fig. 5 Four-stage trajectory.

This result coincides, as it should, with that of the planar two-dimensional homicidal chauffeur game, into which our three-stage game degenerates when $\omega_s \to \infty$.

One should note, however, that there is no switching surface in this particular case, and τ_1 elapses into τ_s, i.e. [see Eq. (35)],

$$\lim_{\omega_s\to\infty} \omega\tau_1 = \frac{\pi}{2} \tag{41}$$

For $\omega_s \to \infty$, the coefficients a_1 and b_1 degenerate into (see Ref. 3)

$$a_1 = 1 - \cos\tau_B, \qquad b_1 = 0 \tag{42}$$

Substitution of Eqs. (36), (38), and (40–42) into Eq. (33) finally yields the known result (Ref. 1, p. 237) for the capture radius of the homicidal chauffeur game:

$$l_c = \gamma \sin^{-1}\gamma + \sqrt{1-\gamma^2} - 1 \tag{43}$$

for l_c and γ satisfying

$$l_c^2 + \gamma^2 \le 1 \tag{44}$$

The above limiting inequality relating γ and l_c may also be obtained directly by setting $\epsilon = 0$ in Eq. (24).

C. Four-Stage Trajectory

In the case where the pursuer's maximum available roll rate is less than ω_m, the optimal maneuver consists of four distinct stages; the first stage starts at $(x_1, 0, 0)$ and terminates at $(x_{s_1}, y_{s_1}, z_{s_1})$ on a u-switching line, the second stage starts at $(x_{s_1}, y_{s_1}, z_{s_1})$ and terminates at $(x_{s_2}, y_{s_2}, z_{s_2})$ on a ω_s-switching line, and the third stage (a short-time tributary) starts at $(x_{s_2}, y_{s_2}, z_{s_2})$ and ends on the $Z = 0$ plane (pursuer's wing plane) at $(x_A, y_A, 0)$; although exhibiting a discontinuity in the gradient (i.e., in the costate variables), the fourth stage continues along a segment of a (u, ω_s) universal line (UL) and reaches the BUP at $(x_f, y_f, 0)$ (see Fig. 5).

The additional (u, ω_s)-UL segment appears as a straight line in our reduced space, the parametric equations of which are

$$x = x_f + (1-\gamma^2)\tau, \qquad y = y_f - \gamma\tau\sqrt{1-\gamma^2}, \qquad z = 0 \tag{45}$$

Once the evader has reached the pursuer's wing plane (i.e., the point x_A, y_A, 0), he or she tends to stay on it, thus taking advantage of the fact that the pursuer has no yaw rate. At this very point the evader changes his or her controls abruptly from the previous values to the final constant values, such that:

$$\lambda_{x_f} = \gamma = \cos\psi_f, \qquad \lambda_{y_f} = \sqrt{1-\gamma^2} = \sin\psi_f$$
$$\lambda_{z_f} = 0 = -\sin\theta_f \tag{46}$$

The assumption of a continuity in the components of the gradient at $(x_A, y_A, 0)$ results in an ambiguity in defining the proper signs of the pursuer's controls (u, ω_s) at τ_A^+. Note that along the UL segment,

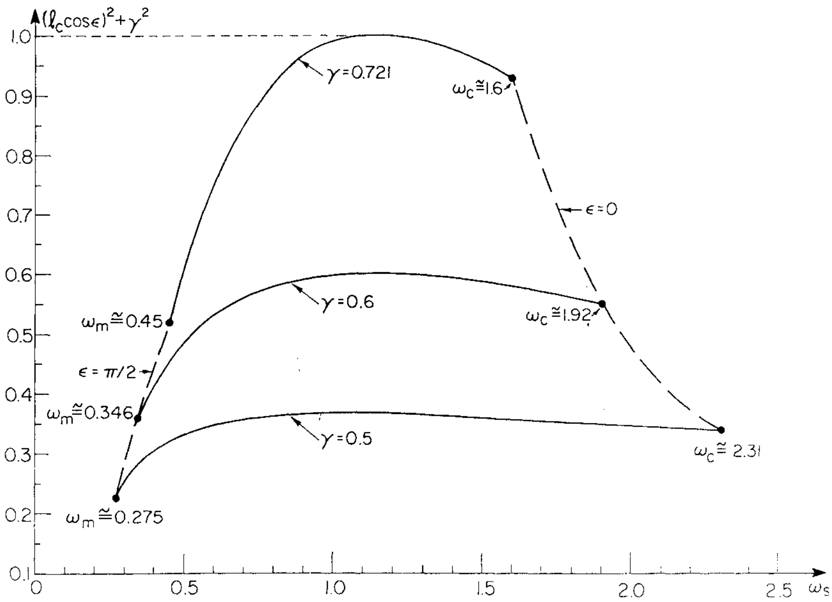

Fig. 6 Criterion for tangential termination of barriers on target set.

i.e., for $0 \le \tau \le \tau_A^-$, these two controls as well as the switching functions and their derivatives are identically zero. Thus, in order to obtain well-defined controls, one has to enforce nonvanishing values for the switching functions at τ_A^+, which suggests that the gradient is discontinuous there. Nevertheless, it should be mentioned that unlike in classical optimal control (see, e.g., Ref. 6, p. 101) the Hamiltonian remains continuous in the present zero-sum game. The gradient discontinuity is finite. However, we do not know a priori anything about its magnitude. In this case it is therefore easier to solve the game in the forward-time sense (i.e., in real time), replacing τ by $-t$ in Eqs. (17) and (18) and changing respectively the initial conditions. We thus start at $(x_1, 0, 0)$ with $\lambda_{x_1} = 0$ according to Eq. (21) and evaluate the costate variables as

$$\lambda_{z_1} = \frac{\gamma}{x_1} = -\sin\theta_0, \qquad \lambda_{y_1} = \cos\theta_0 \tag{47}$$

according to Eqs. (14–16), where θ_0 is the evader's initial pitch control (note that the evader's initial yaw control ψ_0 is equal to $\frac{1}{2}\pi$, which follows from $\lambda_{x_1} = 0$ for $\frac{1}{2}\pi > \theta_0 > 0$). The first switching time t_{s_1} (which annuls the switching function S_1) satisfies the following implicit relation:

$$t_{s_1} = \{\omega_s(\sin 2\theta_0 - \gamma\omega^2 \sin\theta_0)\cos\omega t_{s_1} - \omega(\gamma\omega^2\omega_s\cos\theta_0 + \sin^2\theta_0)\sin\omega t_{s_1} - (\gamma\omega^2\sin\theta_0 + \omega_s\sin 2\theta_0)\}\big/ [\omega\omega_s^2(\omega\sin^2\theta_0\cos\omega t_{s_1} + (\omega_s/2)\sin^2\theta_0\sin\omega t_{s_1})] \tag{48}$$

where $\omega_s = \omega_{s,\max}$. The second switching time t_{s_2} (i.e., the additional time, after t_{s_1}, that annuls the switching function S_2) must also satisfy

$$t_{s_2} = \{[\omega^2 S_3(t_{s_1}) - \omega_s b_{s_1}]\sin\omega t_{s_2} - [\omega S_2(t_{s_1}) + \omega_s a_{s_1} - c_{s_1}] \times \cos\omega t_{s_2} - \omega_s[\omega\omega_s S_2(t_{s_1}) - a_{s_1}]\}\big/[\omega\omega_s\lambda_z(t_{s_2})] \tag{49}$$

where

$$S_3 \stackrel{\Delta}{=} \lambda_y x - \lambda_x y \tag{50}$$

and $a_{s_1}, b_{s_1}, c_{s_1}$ are constants that depend on the transversality conditions at t_{s_1}. The switching time t_{s_2}, according to Eq. (49), is a function of t_{s_1}, which in itself, according to Eq. (48), is a function of θ_0.

The third switching time t_{s_3} is actually a short period of time during which the pursuer flies with an inverted maximum roll rate (i.e., $\omega_s = -\omega_{s,\max}$) while keeping the previous pitch rate. This time can be shown to satisfy the following implicit relationship:

$$t_{s_3} = \frac{A_{s_2}\sin\omega t_{s_3} - (B_{s_2} + 1/\omega^2)\cos\omega t_{s_3} + 1/\omega^2}{\gamma\lambda_z(t_{s_3})} \tag{51}$$

where, again, A_{s_2} and B_{s_2} are constants depending on the transversality conditions at t_{s_2}. After a total time period of $t_{s_1} + t_{s_2} + t_{s_3}$, the $Z = 0$ plane is reached, and an abrupt change in the attitude control is executed by the evader. Starting from $(x_A, y_A, 0)$ and onward the dynamic system is steered along the (u, ω_s) universal line (45) during a time interval t_A until the target set is reached. It can easily be shown that t_A and l_c satisfy

$$t_A = x_A - \left(\gamma/\sqrt{1-\gamma^2}\right)y_A \tag{52}$$

$$l_c = \gamma x_A + \sqrt{1-\gamma^2}\,y_A \tag{53}$$

In order to get a complete solution for the four-stage game, θ_0 has to be found, after which all other values given, for example, by Eqs. (47–53) (which all depend on θ_0), can be calculated. The procedure of finding θ_0 may utilize any numerical or variational method that can determine the extremum value of l_c with respect to θ_0.

If the pursuer is hampered by a very small roll rate (actually $\omega_s \to 0$) it can be shown (for the sake of brevity, only the final results are presented here) that

$$\lim_{\omega_s\to 0} t_{s_1} = \lim_{\omega_s\to 0} t_{s_2} = \frac{\pi}{2} \tag{54}$$

$$\lim_{\omega_s\to 0} t_{s_3} = (\pi - 2)\omega_s^2 \tag{55}$$

$$\lim_{\omega_s\to 0}(\omega_s t_A) = \lim_{\omega_s\to 0}(\omega_s x_A) = \lim_{\omega_s\to 0}(\omega_s x_1) = \gamma \tag{56}$$

$$\lim_{\omega_s\to 0} y_A = \gamma(\pi - 2)$$

and finally,

$$\lim_{\omega_s\to 0}(\omega_s l_c) = \gamma^2 \tag{57}$$

Thus, for vanishingly small roll rates the capture radius is large and is proportional to $1/\omega_s$ with a proportionality constant being just the squared speed ratio γ^2. Graphs of l_c and x_1 (the initial separation) as a function of $0 < \omega_s < \infty$, for different values of γ, are shown in Figs. 7 and 8, respectively.

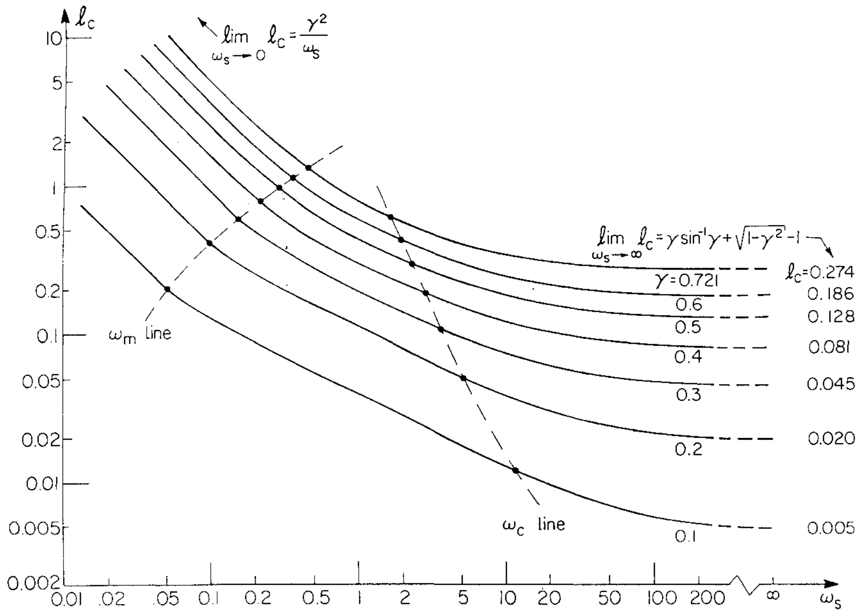

Fig. 7 Capture radius vs roll rate for different values of γ.

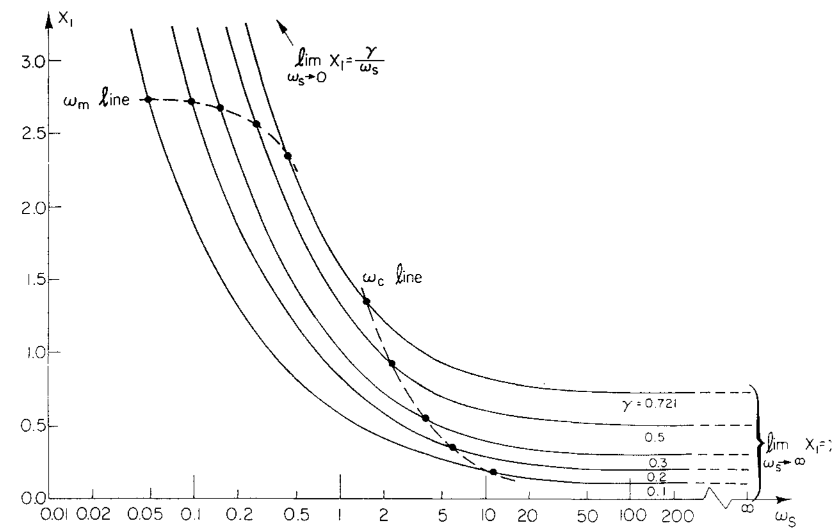

Fig. 8 Initial separation x_1 vs roll rate for different values of γ.

V. Numerical Examples

The two following examples are based on the results depicted in Fig. 7. These examples indicate that a low pursuer's roll-to-pitch rate ratio generally leads to a poor (large) miss distance (Example 1). On the other hand, a large roll-to-pitch rate ratio, along with a lower players' speed ratio $\gamma = V_E/V_P$, is shown to improve the miss distance significantly (Example 2).

Example 1 (low roll rate)

$$V_p = 1000 \text{ m/s}, \qquad V_E = 300 \text{ m/s} \qquad (\gamma = 0.3)$$

$$R = 1146 \text{ m}$$

$$\omega_s/(V_p/R) = 1$$

that is,

$$\omega_s \cong 50 \text{ deg/s}$$

The initial (optimal) separation between players is calculated to be (see Fig. 8)

$$x_1/R \cong 1$$

that is,

$$x_1 \cong 1146 \text{ m}$$

and the miss distance is

$$l_c/R \cong 0.2$$

that is,

$$l_c \cong 229.2 \text{ m}$$

Example 2 (large roll rate)

$$V_p = 1000 \text{ m/s}, \qquad V_E = 100 \text{ m/s} \qquad (\gamma = 0.1)$$

$$R = 1146 \text{ m}$$

$$\omega_s/(V_p/R) = 15$$

that is,

$$\omega_s \cong 750 \text{ deg/s}$$

The initial separation in this case (see Fig. 8) is

$$x_1/R \cong 0.168$$

that is,

$$x_1 \cong 192.5 \text{ m}$$

and the miss distance (see Fig. 7) is determined as

$$l_c/R \cong 0.01$$

that is,

$$l_c \cong 11.5 \text{ m}$$

It should be noted that the miss distances presented in Fig. 7 should be considered only as upper bounds, which is a direct consequence of the fact that the evader has unlimited maneuverability. Actually, for a more "realistic" evader, an "optimal" pursuer will always achieve smaller miss distances than those appearing in Fig. 7.

VI. Summary and Conclusions

An analytic solution is presented for the dimensionless capture radius (normalized with respect to the pursuer's radius R) in terms of the nondimensional pursuer's roll rate (normalized with respect to V_p/R) for different values of players' speed ratio $\gamma = V_E/V_p \leq 0.721$. The solution for $0.721 < \gamma < 1$ will be given in a forthcoming paper. It is shown that for some initial separation X_1 a faster pursuer can steer the dynamic system into the target set (thus guaranteeing unconditional capture) by executing a two-, three-, or four-stage maneuver, depending on the relative magnitude of his or her available roll rate.

There exists a critical value of the roll rate above which the optimal game consists of three different trajectories and below which there are only two. The two stages are characterized by two hard turns (maximum pitch rate) of the pursuer in opposite directions, whereas the evader is maintaining his or her course direction. The pursuer simultaneously employs his or her maximum roll rate in the same direction. The critical roll rate is determined by the limiting value of the BUP angle, i.e., $\epsilon = 0$. For example, the nondimensional value of the critical roll rate for a speed ratio of $\gamma = V_E/V_p = 0.5$ is $\omega_c = 2.31$.

For values of ω_s larger than ω_c, the optimal game leading to the BUP consists of three stages, where in addition to the previous two stages the pursuer employs a zero roll-rate ($\omega_s = 0$) hard turn just prior to reaching the target set. Along the third stage, which is in fact a ω_s universal line, the pursuer maintains the same pitch rate as in the second stage. Thus, for $\omega_s > \omega_c$ the pursuer is capable of steering the end game into a two-dimensional plane that is his or her preferable pitch plane. In many realistic pursuit-evasion situations it is desirable to force the evader into the pitch plane just prior to game termination. Therefore, the analytic value of ω_c reported here may serve useful for the optimal design of roll/pitch controllers of a bank-to-turn missile for a prescribed miss distance and speed ratio.

In addition to the critical roll rate that renders a continuous transition from a two- to a three-stage maneuver, there also exists a marginal roll rate below which the evader is capable of steering the end game into the "unfavorable" pursuer's yaw plane. This marginal roll rate, here denoted by ω_m, is determined from the limiting value of the BUP angle, i.e., $\epsilon = \frac{1}{2}\pi$. As an example, for $\gamma = 0.5$ we find that $\omega_m \cong 0.275$ where the minimum miss distance is $l_c \cong 0.96$. This value should be compared against the minimum capture radius of $l_c \cong 0.3$ obtained at $\omega_s = \omega_c = 2.31$.

Increasing the roll rate indefinitely ($\omega_s \to \infty$) reduces the formulation into the homicidal chauffeur game, which is a one-stage maneuver in which the faster pursuer uses his or her maximum pitch rate while executing a zero-roll maneuver. Under these conditions the present capture criterion degenerates into the well-known two-dimensional Isaacs criterion that for $\gamma = 0.5$ renders $l_c \cong 0.128$. Thus, increasing the roll rate in the range $\infty > \omega_s > \omega_m$ tends to decrease the capture radius, where the smallest value is given by the homicidal chauffeur criterion and the maximum value is attained at $\omega_s = \omega_m$. Below the marginal roll rate ω_m, the game consists of four distinct stages.

References

[1]Isaacs, R., *Differential Games*, R. E. Krieger Pub. Co., New York, 1975.

[2]Miloh, T., "A Note on Three-Dimensional Pursuit Game with Bounded Curvature," *IEEE Transactions on Automatic Control*, Vol. 27, 1982, p. 739.

[3]Miloh, T., Pachter, M., and Segal, A., "The Effect of a Finite Roll-Rate on the Miss-Distance of a Bank-to-Turn Missile," *Computers and Mathematics with Applications*, Vol. 26, No. 6, 1993, p. 43.

[4]Breakwell, J. V., and Merz, A. W., "Minimum Required Capture Radius in Coplanar Model of the Aerial Combat Problem," *AIAA Journal*, Vol. 15, 1987, p. 1089.

[5]Miloh, T., "The Game of Two Ellipsoidal Ships," *Optimal Control Applications and Methods*, Vol. 4, 1983, p. 13.

[6]Bryson, A. E., Jr., and Ho, Y.-C., *Applied Optimal Control*, Hemisphere, New York, 1975.